The effect of the noncentral impurity-matrix interaction upon the thermal expansion and polyamorphism of solid CO–C$_{60}$ solutions at low temperatures

A.V. Dolbin, V.B. Esel'son, V.G. Gavrilko, V.G. Manzhelii, and N.A. Vinnikov

B. Verkin Institute for Low Temperature Physics and Engineering of the National Academy of Sciences of Ukraine
47 Lenin Ave., Kharkov 61103, Ukraine
E-mail: dolbin@ilt.kharkov.ua

G.E. Gadd, S. Moricca, and D. Cassidy

Australian Nuclear Science and Technology Organization, NSW 2234, Australia

B. Sundqvist

Department of Physics, Umea University, SE - 901 87 Umea, Sweden

Orientational glasses with CO molecules occupying 26 and 90% of the octahedral interstitial sites in the C$_{60}$ lattice have been investigated by the dilatometric method in a temperature interval of 2.5–22 K. At temperatures 4–6 K the glasses undergo a first-order phase transition which is evident from the hysteresis of the thermal expansion and the maxima in the temperature dependences of the linear thermal expansion coefficients $\alpha(T)$, and the thermalization times $\tau_1(T)$ of the samples. The effect of the noncentral CO–C$_{60}$ interaction upon the thermal expansion and the phase transition in these glasses was clarified by comparing the behavior of the properties of the CO–C$_{60}$ and N$_2$–C$_{60}$ solutions.

Introduction

Below T = 90 K fullerite C$_{60}$ transforms into an orientational glass. According to dilatometric and x-ray structural data [1–7], the gases dissolved in C$_{60}$ produce a significant effect on the thermal expansion of the glass and cause a first-order phase transition (polyamorphism) in it. It is interesting to find out how particular molecular parameters of the admixture gas can influence the properties of C$_{60}$ lattice as a result of a impurity–matrix interaction. To judge accurately the effect of varying a certain molecular parameter, the gas impurities should be chosen so that they differ mainly in this particular parameter, whilst other molecular parameters that may have an effect on the C$_{60}$ lattice are essentially kept the same. For example, we would like to probe the effect on the impurity–matrix interaction of altering the electronic charge distribution within a diatomic gas. The choice of a homo and

hetero diatomic gas with similar molecular bond lengths would be a good starting point for investigating this important question. We have conveniently chosen CO–C$_{60}$ and N$_2$–C$_{60}$ solutions. In contrast to O$_2$, CO and N$_2$ molecules do not react chemically with C$_{60}$ at the temperatures to which C$_{60}$ has to be heated to desorb volatile impurities. These molecules also have practically identical molecular weights (M(CO) = 28.0105, M(N$_2$) = 28.0134) as well as comparable gas-kinetic diameters (σ(CO) = = 3.766 Å, σ(N$_2$) = 3.756 Å) [8], but they differ significantly in electric quadrupole moments Q (Q(CO) = = –2.839·10^{-26} esu, Q(N$_2$) = – 1.394·10^{-26} esu) [9]. N$_2$ also does not have a dipole moment whereas CO does. However, as will be discussed further on, it is the quadrupole moment and not the dipole moment, that contributes most to the effect that these impurities have upon

the low-temperature thermal expansion and polyamorphism of C_{60}.

The dilatometric data on orientational C_{60} glasses with molar N_2 concentrations (N_2-to-C_{60} molecule ratio) of 9.9 and 100% has previously been published in Ref. 3, so that this paper extends the studies to include those from CO–C_{60} solutions, followed by comparison of the two data sets.

In this study, we investigate the impurity effect of CO on the properties and phase transformations of orientational C_{60} glasses. Solutions of CO–C_{60} with both 26 and 90 mol. % CO, were investigated.

The impurity (N_2, CO) molecules occupy the octahedral interstitial cavities in the C_{60} lattice, of which there is effectively one octahedral cavity per C_{60} molecule. As a result of this, the molar CO and N_2 concentrations are equal to the N_2 and CO occupancies of the octahedral sites in the C_{60} lattice.

Samples and measuring technique

The C_{60} sample with 26 mol. % CO was prepared as follows. Prior to saturation with CO, the sample, which was a pressed cylinder of solid C_{60} powder, 9 mm high and 10 mm in diameter (prepared by a procedure as described in Ref. 2), was kept for 72 hours under dynamic evacuation to remove gas impurities ($P = 1 \cdot 10^{-3}$ mm Hg, $T = 400$ °C). The outgassed sample and cell, was filled with CO gas at room temperature to a pressure of 760 mm Hg and sealed. The sample was kept under these sealed conditions for 105 days.

The thermal expansion of the CO–C_{60} solutions was investigated using a low-temperature capacitance dilatometer. Its design and the measurement technique are detailed in Ref. 14.

Immediately before the dilatometric measurement, the measuring cell with the CO–C_{60} sample and which was filled with CO, was cooled slowly to 65 K, which is just below the freezing point of CO at 68 K. The cell was evacuated at this temperature to remove the condensed CO, that was CO that had not been absorbed by the sample. The sample was pumped on further until a base pressure of $1 \cdot 10^{-5}$ mm Hg was attained, followed by cooling of the sample to the base temperature of 4.2 K. The thermal expansion of the CO–C_{60} sample was measured after a four-hour exposure to this temperature.

After measuring the thermal expansion of the sample, the amount of gas impurities and their compositions were determined qualitatively and quantitatively using a vacuum desorption gas analyzer [12]. It was found that about 26% of the octahedral cavities of the C_{60} lattice were occupied by CO. Most of the CO was desorbed on heating the sample to 300 °C (Fig. 1). The preparation and analysis techniques for the C_{60} sample with 90 mol. % CO are described in Ref. 13.
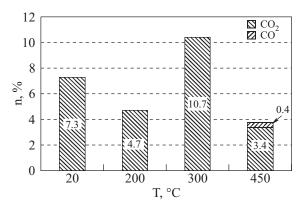

Fig. 1. The composition of the gas mixture (in percentage of occupation of the octahedral cavities) desorbed from the C_{60} sample with 26 mol. % CO on stepwise heating the sample to $T = 450$ °C.

Results and discussion

The temperature dependences of the linear thermal expansion coefficient (LTEC) $\alpha(T)$ of pure C_{60} and of the C_{60} samples with different contents of the CO impurity are shown in Fig. 2. The $\alpha(T)$ values are averaged over several measurement series. Owing to the cubic symmetry of their lattices, the thermal expansion of the samples can be described with a single LTEC.

The thermal expansion of the investigated samples exhibited a number of specific features. On heating (curves *1*, *2*) and subsequent cooling (curves *3*, *4*) the thermal expansion coefficient has a hysteresis which points to a first-order phase transition in the orientational CO–C_{60} glasses. No hysteresis was observed for pure C_{60} (curve *5*). From the two different CO–C_{60} samples, it appears that the onset of the hysteresis shifts towards higher temperature with increased impurity concentration, shifting from 3 K for the 26 mol. % CO to 4 K for the 90 mol. % CO. Within the temperature range starting from the lowest measured temperature of 2.5 K to the respective hysteresis onset temperatures, it is found that the $\alpha(T)$ for a particular sample are practically identical for both the heating and cooling curves. Moreover, the LTECs of both the CO–C_{60} samples (26 and 90 mol. % CO) and that of pure C_{60} also coincide within the measurement error. On heating in the interval 4–6 K there is a region of instability with higher experimental errors and local LTEC maxima (Fig. 2), however, the errors are appreciably lower than the maxima heights observed. It is assumed [3–5] that within this interval of temperatures, occurs the first-order phase transition between the two differing impurity doped orientational glasses.

Previous investigations [1–5] show that the thermal expansion of gas-doped C_{60} contains positive and negative components with different characteristic relaxation times (τ_1 and τ_2, respectively). With a temperature
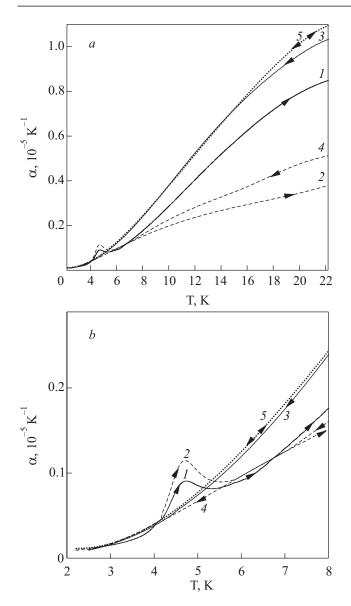
Fig. 2. The temperature dependence of the linear thermal expansion coefficient of CO–C$_{60}$ solutions in temperature intervals 2.5–22 (*a*) and 2.5–8 (*b*) K. The curves *1* and *2* are from heating the 26 and 90 mol. % CO–C$_{60}$ samples, respectively, whilst curves *3* and *4* are from cooling the 26 and 90 mol. % CO–C$_{60}$ samples, respectively. The dotted line (*5*) is from pure C$_{60}$ by either heating or cooling the sample.

Fig. 3. The temperature dependences of the positive and negative components of the thermal expansion coefficient of CO–C$_{60}$ solutions as studied in the intervals of 2.5–22 (*a*) and 2.5–8 (*b*) K. The positive contributions are the labelled curves *1* — 26 mol. % CO and *2* — 90 mol. % CO, whilst the negative contributions are labelled as the curves *3* — 26 mol. % CO and *4* — 90 mol. % CO. Pure C$_{60}$ which only exhibits a positive contribution is shown as a dotted line (*5*).

change of the sample, the positive component is attributed [1–5] to the process of temperature equalization over the bulk sample (thermalization), whilst the negative component accounts orientational changes of the C$_{60}$ molecules induced by the temperature change of the sample. Since a C$_{60}$ crystal is perceived as consisting of domains of different orientational orders of the C$_{60}$ molecules, and with these domains in a particular crystal separated by interlayers of C$_{60}$, it has been concluded theoretically [15–17] that the negative component of the thermal expansion observed at these low temperatures
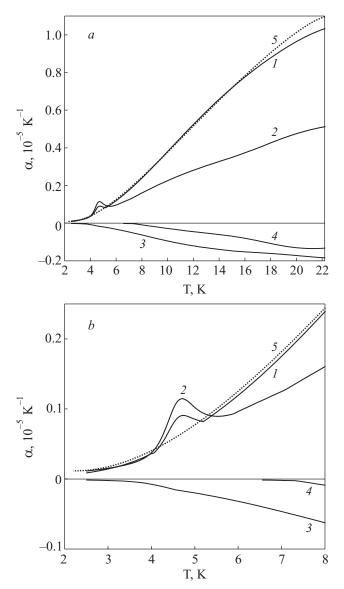
studied, results from the C$_{60}$ reorientation within these actual interlayers and not in the domains themselves.

The thermal expansion of C$_{60}$ samples doped with CO also has two components. They were separated in a similar fashion to the techniques described in Ref. 1. The temperature dependences of the positive and negative components for samples with different CO concentration are illustrated in Fig. 3.

It is seen from Fig. 2,*b* that all the LTEC curves are lower than the LTEC of pure C$_{60}$ over this temperature range, with the heating and cooling curves of the 90 mol. %

CO and the heating curve of the 26 mol. % CO, being markedly lowered. From Fig. 2,*b* we can conclude that this lowering scales with increases in the concentration of the CO impurity. Above 8 K, although the heating and cooling LTEC curves for the 90 mol. % CO and the heating curve of the 26 mol. % CO appear lowered even further than the corresponding LTEC curve of pure C$_{60}$, the cooling curve of the 26 mol. % CO is more or less identical with that of pure C$_{60}$. However if we consider just the positive component to this curve, as shown in Fig. 3, it is seen to also be lower than that of pure C$_{60}$ (which only exhibits a positive component). In N$_2$–C$_{60}$ solutions this lowering effect of the LTEC curves, exists only at high N$_2$ concentrations and is much less [3]. This lowering effect is explained as follows. Over the temperature range spanned in our experiments (2.5–22 K), the thermal expansion of pure C$_{60}$ is determined by the changes with temperature that occur in a range of phenomena, which predominantly include the translational lattice vibrations, the C$_{60}$ librations and the soft modes and two-level systems of the C$_{60}$ glasses, and in particular those associated with the changing of the relative orientations of the C$_{60}$ molecules with respect to each other. The admixed gas molecules within the octahedral sites can affect the above contributors as well as making their own contribution to the thermal expansion of the solid CO–C$_{60}$ solution, through its own thermal motions.

As noted above, the thermal expansion coefficients of pure C$_{60}$ and the CO–C$_{60}$ solutions coincide at the lowest temperatures of the experiment. This means that at these temperatures the CO impurity has little effect on the dominant contributors to the thermal expansion that being the translational lattice vibrations, the two-level systems and the soft modes [18]. The weak effect of the impurity on the translational vibrations of the C$_{60}$ lattice is quite natural because CO adds little to the effective molecular weight of the CO–C$_{60}$ solutions and changes the lattice constant of C$_{60}$ at most by 0.15 % [19]. As the temperature rises, the contributions of the C$_{60}$ librations and the motions associated with the CO molecule (translational, rotational and internal vibrational) increase significantly. But any contribution from the CO through its increased thermal motion can only lead to higher LTEC values. Therefore, the lower LTECs of the CO–C$_{60}$ solutions in comparison with those of pure C$_{60}$ must be attributed to the diminished contribution of the C$_{60}$ librations. This arises from the fact that the CO molecules at $T \leq 77$ K are oriented in a particular fashion within the octahedral interstitial sites of C$_{60}$ [11,20,21] so that there is a noncentral interaction between the impurity and the surrounding C$_{60}$ molecules and which is not nullified by any rotation of the CO molecules within the sites. The CO molecule has both dipole and quadruple electrical moments although the dipole moment is rather weak [22], so

that the noncentral CO–C$_{60}$ interaction is mainly determined by the quadrupole moment of the CO molecule. This CO orientational induced noncentral force interaction acting on the C$_{60}$ molecules tends to increases the frequency of their librations. As a result, the contribution of the C$_{60}$ librations to the positive component of the thermal expansion for these CO–C$_{60}$ solutions, and over the studied temperature range, is reduced as compared to that of the pure C$_{60}$ sample. Only at higher temperatures will their effect be realized as their contribution increases with temperature as they become more and more thermally activated. This effect is weaker for the N$_2$–C$_{60}$ solutions as the quadrupole moment of N$_2$ molecules is much smaller and this is clearly seen in Fig. 4 that compares the positive and negative components of the thermal expansion for samples with 90 mol. % CO and 100 mol. % N$_2$. We have chosen these two samples to compare, because the effects of impurities upon the thermal expansion of doped fullerites are most evident at their high concentrations.

In the context of the above consideration, the negative component of the thermal expansion is determined by the probability of reorientation of the C$_{60}$ molecules in the domain interlayers. It is found that the magnitude of the negative component of the LTEC for the CO–C$_{60}$ solutions decreases considerably as the CO concentration increases from 26 to 90% (Fig. 3). The absence of a negative component in the thermal expansion of pure C$_{60}$ prompts us to conclude that on dissolution of CO in the C$_{60}$ lattice, the probability of C$_{60}$ reorientation in the do-
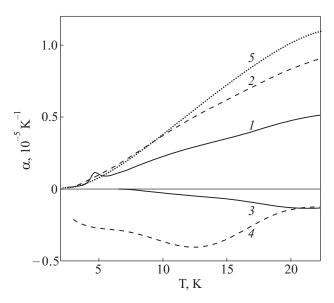

Fig. 4. The temperature dependences of the positive and negative components of the linear thermal expansion coefficient are shown for both CO–C$_{60}$ (solid lines) and N$_2$–C$_{60}$ (dashed lines) [3] solutions. The positive components are the curves *1* — 90 mol. % CO and *2* — 100 mol. % N$_2$, whilst the negative components are the curves *3* — 90 mol. % CO and *4* — 100 mol. % N$_2$. Again pure C$_{60}$ which only has a positive contribution is shown as the dotted line (*5*).

main interlayers must first increase with impurity concentration up to a certain impurity concentration but increasing the impurity concentration past this, it must start to decrease again and Fig. 3 even suggests it contribution is reduced to zero contribution at 100% occupancy with CO. By contrast, for N_2–C_{60} solutions, in which the noncentral interaction between the N_2 and the C_{60} molecules is weaker, there is an opposite trend with the negative contribution to the thermal expansion being much greater at higher N_2 concentrations than at lower ones. It should be noted that a change from a low to a high impurity concentration will reduce the temperature interval of the negative contribution for the CO–C_{60} solution but in contrast increases it for the N_2–C_{60} solution [3].

It is of our opinion that these observations of the thermal expansion behavior for the CO–C_{60} and N_2–C_{60} solutions suggests that in both cases, there is a competition between two contrasting mechanisms. On the one hand, we have the CO and N_2 impurities introduced into the interstitial sites of C_{60} pushing the neighboring C_{60} molecules farther apart. This mechanism tends to reduce the effect from the noncentral interaction between the C_{60} molecules but promote their reorientation. This increases the negative contribution to the thermal expansion. On the other hand, their introduction also results in a noncentral interaction between the impurity and the neighboring C_{60} molecules that reduces the probability of C_{60} reorientation and decreases the negative contribution to the thermal expansion. The first mechanism dominates in the N_2–C_{60} solutions while the other prevails in the CO–C_{60} solutions with high CO concentrations.

It is expected that the noncentral interaction between the impurity and C_{60} matrix can affect the characteristic time of C_{60} reorientation (τ_2) within the interlayers between the domains. As seen in Fig. 5, the τ_2 values have
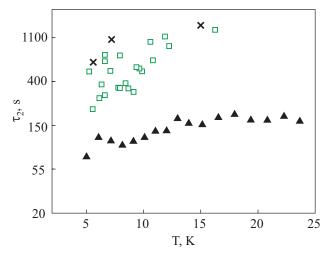
been extracted from the negative component of the LTEC are much longer for the CO–C_{60} solution than for the N_2–C_{60} one, indicating that the CO molecules with the substantially larger quadrupole moment than that of N_2 greatly depress on account of this enhanced noncentral CO–C_{60} interaction, the probability of C_{60} reorientation.

The local maxima in the temperature dependences of the positive components of the LTECs for the CO–C_{60} samples may indicate that within the interval of 4–5,5 K occurs the temperatures associated with the phase transformations between the orientational CO–C_{60} glasses. This assumption is supported by the analysis of the temperature dependences of the relaxation time $\tau_1(T)$ associated with thermal equilibration of the CO–C_{60} solution, and obtained from the positive component of the LTEC. As shown in Fig. 6, this extracted thermalization time τ_1 of the sample, increases sharply in the temperature interval of the local LTEC maxima because the heat supplied to the sample during heating is partially consumed by the phase transformation in the orientational glass.

In contrast to the CO–C_{60} solutions, the dependences $\alpha(T)$ and $\tau_1(T)$ of the N_2–C_{60} solution have no distinct maxima. The glasses coexisting in gas–fullerites solutions differ only in the orientational order of the C_{60} molecules [2,15–17]. Since the noncentral interaction between the impurity and matrix molecules is stronger in the CO–C_{60} solution, we can assume that the latent heat of the phase transformation between the glasses and associated with this change in the orientational order is much larger for this solution, up as maxima in the $\alpha(T)$ and $\tau_1(T)$ plots.

It is known that gas impurities of high concentrations can often cause microcracking and even fracture of the C_{60} samples [2,3,5,23]. The higher τ_1 values for the sample with the high CO concentration can be attributed to
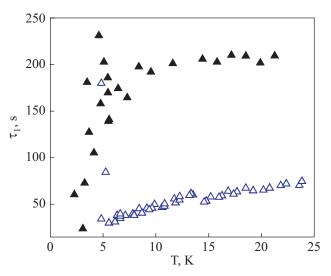

Fig. 5. The characteristic time τ_2 for C_{60} reorientation extracted from the negative components of the thermal expansion: CO–C_{60} with 90 (✕) and 26 (□) mol. % CO; and N_2–C_{60} with 100 mol. % N_2 (▲).

Fig. 6. The characteristic times τ_1 of the positive components of thermal expansion from 90 (▲) and 26 (△) mol. % CO–C_{60}.
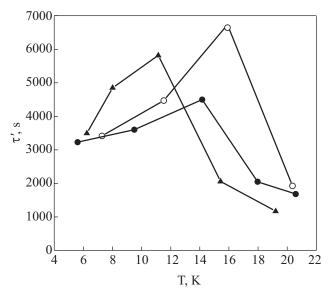
Fig. 7. The temperature dependences of the characteristic time τ' for the phase transformation between the orientational glasses for N$_2$–C$_{60}$ with 100 mol. % N$_2$ (▲, [3]) and for CO–C$_{60}$ with 26 (○) and 90 (●) mol. % CO.

evidence for microcracks occurring within such samples. Such an occurrence will increase the thermal resistance and hence the characteristic time of thermalization τ_1.

The phase transformation in the CO–C$_{60}$ samples was investigated by conducting a series of experiments involving thermocycling of the samples at $T > 5.5$ K. The thermocycling was performed in several narrow intervals, with the step being no more than 2 K. The experimental technique and data processing have been detailed elsewhere [2,3]. In the course of the thermocycling, the hysteresis loop was found to narrow gradually (from cycle to cycle) and in doing so the negative component of the thermal expansion decreased until the LTECs measured on heating were approaching those obtained on cooling. The process of thermocycling thus brought the system to a more advantageous thermodynamic state between the co-existing glasses. The characteristic times τ' of this process are shown in Fig. 7 as a function of the average thermocycling temperature.

It is interesting that the dependences $\tau'(T)$ are similar qualitatively for all three samples, although the $\tau'(T)$ maxima for the CO–C$_{60}$ solutions are shifted towards a higher temperatures. Currently, the lack of information concerning the actual distinctions between the orientational glasses coexisting in the CO–C$_{60}$ and N$_2$–C$_{60}$ solutions, impedes any further analysis of the temperature dependences of $\tau'(T)$ for these systems.

Conclusions

A first order phase transition was observed in the orientational C$_{60}$ glasses at liquid helium temperatures, during dilatometric investigations on two CO–C$_{60}$ solu-

tions with 26 and 90 mol. % CO. The phase transformation revealed itself through observation of a hysteresis in the thermal expansion, the occurrence of local maxima in the temperature dependence of the linear thermal expansion coefficients, and lastly by a maximum in the temperature dependence of the thermalization time τ_1 of the investigated systems. From the temperature range of the observed maxima in the thermal expansion, the phase transitions in the orientational glasses of the CO–C$_{60}$ solutions is believed to occur in the interval 4–6 K.

The thermal expansion of the CO–C$_{60}$ solutions is a sum of positive and negative components and each with the characteristic relaxation times τ_1 and τ_2, respectively. τ_1 is the time of temperature equalization over the sample (thermalization) whilst τ_2 specifies the time of C$_{60}$ reorientation in the interdomain space within the CO–C$_{60}$ crystallites.

We compared the thermal expansion of CO–C$_{60}$ and N$_2$–C$_{60}$ solutions in which the impurity molecules have close gas-kinetic diameters and molecular weights, but where CO has a considerably larger quadrupole moment than N$_2$.

Because of the stronger noncentral interaction between the interstitial CO and the neighboring C$_{60}$ molecules, the CO–C$_{60}$ solution has some specific features that distinguish it from the N$_2$–C$_{60}$ solution. These are:

i) The linear thermal expansion coefficients (LTECs) are lower in the «high-temperature» phase in comparison with the LTECs of pure C$_{60}$. This is because the frequencies of C$_{60}$ librations are increased through this noncentral interaction and their contribution to the LTECs shifts to temperatures above the T interval of the experiment.

ii) The dependences $\alpha(T)$ and $\tau_1(T)$ have maxima in the temperature interval of phase transformation. No maxima were detected in the N$_2$–C$_{60}$ solutions.

iii) The C$_{60}$ molecules have much longer reorientation times τ_2, which is an obvious consequence of the enhancement of the noncentral interaction between the impurity and matrix molecules.

iv) There is a change in the concentration dependence of the negative contribution to the LTEC. Two contrasting mechanisms are responsible for these observations associated with the negative LTEC contribution. On the one hand, impurities increase the spacings between the C$_{60}$ molecules which depresses their noncentral interaction and increases the probability of their reorientation. On the other hand, the noncentral interaction between the impurity and matrix molecules decreases the probability of C$_{60}$ reorientation. The first mechanism is dominant in the N$_2$–C$_{60}$ solutions, whilst the other predominates in the CO–C$_{60}$ solutions with higher CO concentrations.

1. A.N. Aleksandrovskii, A.S Bakai, A.V. Dolbin, V.B. Esel'son, G.E. Gadd, V.G. Gavrilko, V.G. Manzhelii, S. Moricca, B. Sundqvist, and B.G. Udovidchenko, *Fiz. Nizk. Temp*. **29,** 432 (2003) [*Low Temp. Phys*. **29**, 324 (2003)].

2. A.N. Aleksandrovskii, A.S. Bakai, D. Cassidy, A.V. Dolbin, V.B. Esel'son, G.E. Gadd, V.G. Gavrilko, V.G. Manzhelii, S. Moricca, and B. Sundqvist, *Fiz. Nizk. Temp*. **31**, 565 (2005) [*Low Temp. Phys*. **31**, 429 (2005)].

3. V.G. Manzhelii, A.V. Dolbin, V.B. Esel'son, V.G. Gavrilko, D. Cassidy, G.E. Gadd, S. Moricca, and B. Sundqvist, *Fiz. Nizk. Temp*. **32**, 913 (2006) [*Low Temp. Phys*. **32**, 695 (2006)].

4. A.V. Dolbin, N.A.Vinnikov, V.G. Gavrilko, V.B. Esel'son, V.G. Manzhelii, and B. Sundqvist, *Fiz. Nizk. Temp*. **33**, 618 (2007) [*Low Temp. Phys*. **33**, 465 (2007)].

5. A.V. Dolbin, V.B. Esel'son, V.G. Gavrilko, V.G. Manzhelii, N.A.Vinnikov, G.E. Gadd, S. Moricca, D. Cassidy, and B. Sundqvist, *Fiz. Nizk. Temp*. **33**, 1401 (2007) [*Low Temp. Phys*. **33**, 1068 (2007)].

6. A.I. Prokhvatilov, N.N. Galtsov, I.V. Legchenkova, M.A. Strzhemechny, D. Cassidy, G.E. Gadd, S. Moricca, B. Sundqvist, and N.A. Aksenova, *Fiz. Nizk. Temp.* **31**, 585 (2005) [*Low Temp. Phys.* **31**, 445 (2005)].

7. B. Sundqvist, *Adv. Physics* **48**, 1 (1999).

8. S. Chapmen and T.G. Cowling, *The Mathematical Theory of Nonuniform Gases*, Cambridge (1939), pp. 225 and 229.

9. C. Graham, D.A. Imrie, and R.E. Raab, *Mol. Phys*. **93**, 49 (1998).

10. B. Renker, G. Roth, H. Schober, P. Nagel, R. Lortz, C. Meingast, D. Ernst, M.T. Fernandez-Diaz, and M. Koza, *Phys. Rev*. **B64**, 205417 (2001).

11. S. Smaalen, R. Dinnebier, I. Holleman, G. Helden, and G. Meijer, *Phys. Rev*. **B57**, 6321 (1998).

12. A.M. Aleksandrovskii, M.A. Vinnikov, V.G. Gavrilko, O.V. Dolbin, V.B. Esel'son, and. V.P. Maletskiy, *Ukr. Fiz. Zh.* **51**, 1150 (2006).

13. G.E. Gadd, S. Moricca, S.J. Kennedy, M.M. Elcombe, P.J. Evans, M. Blackford, D. Cassidy, C.J. Howard, P. Prasad, J.V. Hanna, A. Burchwood, and D. Levy, *J. Phys. Chem. Solids* **58**, 1823 (1997).

14. A.N. Aleksandrovskii, V.B. Esel'son, V.G. Manzhelii, A.V. Soldatov, B. Sundqvist, and B.G. Udovidchenko, *Fiz. Nizk. Temp.* **23**, 1256 (1997) [*Low Temp. Phys*. **23**, 943 (1997)].

15. V.M. Loktev, J.N. Khalack, and Yu.G. Pogorelov, *Fiz. Nizk. Temp.* **27**, 539 (2001) [*Low Temp. Phys.* **27**, 397 (2001)].

16. J.M. Khalack and V.M. Loktev, *Fiz. Nizk. Temp.* **29,** 577 (2003) [*Low Temp. Phys.* **29**, 429 (2003)].

17. A.S. Bakai, *Fiz. Nizk. Temp*. **32**, 1143 (2006) [*Low Temp. Phys*. **32**, 1033 (2006)].

18. M.A. Ramos, C. Talon, R.J. Jimenez-Rioboo, and S. Vieira, *J. Phys.: Condens. Matter* **15,** 1007 (2003).

19. N.N. Galtsov, A.I. Prokhvatilov, G.N. Dolgova, D. Cassidy, G.E. Gadd, S. Moricca, and B. Sundqvist, *Fiz. Nizk. Temp.* **33,** 1159 (2007) [*Low Temp. Phys*. **33**, 881 (2007)].

20. I. Holleman, G. von Helden, E.H.T. Oithof, P.J.M. van Bentum, R. Engeln, G.H. Nachtegaal, A.P.M. Kentgens, B.H. Meier, A. van der Avoird, and G. Meijer, *Phys. Rev. Lett*. **79**, 1138 (1997).

21. I. Holleman, G. von Helden, A. van der Avoird, and G. Meijer, *Phys. Rev. Lett*. **80**, 4899 (1998).

22. M.W. Melhuish and R.L. Scott, *J. Phys. Chem*. **68,** 2301 (1964).

23. L.S. Fomenko, S.V. Lubenets, V.D. Natsik, Yu.E. Stetsenko, K.A. Yagotintsev, M.A. Strzhemechny, A.I. Prokhvatilov, Yu.A. Osipyan, A.N. Izotov, and N.S. Sidorov, *Fiz. Nizk. Temp.* **34**, 86 (2008) [*Low Temp. Phys.* **34**, 69 (2008)].